The Characterization of the Kinematic and Dynamic Properties of the Ankle Joint for an Artificial Ankle Joint Design

Artur Gmerek, Nader Meskin, Ehsan Sobhani Tehrani, and Robert E. Kearney

***Abstract*—The kinematic and dynamic properties of the ankle joint (talocrural region) in normal subjects provide important information for the design of rehabilitation robots, below-knee prostheses, ankle-foot orthoses, and exoskeletons. This paper presents a quantitative analysis of published experimental data, simulation studies of human gait, and a dynamic model of ankle joint intrinsic and reflex stiffness to determine design requirements for such ankle devices to operate in the sagittal plane (i.e. ankle plantarflexion/dorsiflexion). The design requirements are derived in terms of average torque, rotatum, range of motion, velocity, acceleration, system bandwidth, torque-velocity curve, and the torque probability density function.**

I. Introduction

Ankle joint impairments due to joint inflammation, arthritis, sprain, stroke and other neuromuscular diseases is one of the most common reasons for altered gait and problems during walking. According to emergency department records between 2002 and 2006 in the United States the incidence rate of ankle sprain was 2.15 per 1000 persons per year [1]. Also, the National Spinal Cord Injury Statistical Center found in 2014 that there were 12500 new cases of paraplegic each year in the United States alone [2]. Moreover, the Amputee Coalition of America estimated that there are 185000 new lower extremity amputations each year only within the United States [3]. Many of these cases can be treated by short-term rehabilitation, surgery or medication but some would require long-term rehabilitation or assistive devices that could support patients during walking throughout life. These assistive robots for the ankle joint can ameliorate the impact of impairments that affect gait, and therefore, improve the quality of life of those affected.

The assessment of the maximum kinematic and dynamic parameters of the human body is often the first step when designing assistive or rehabilitation robots. Some robots are designed based on only *static* force analysis, and consequently, these robots are either oversized or cannot meet the established *dynamic* requirements. Therefore, it is important to determine both kinematic and dynamic requirements based on experimental gait data and dynamic simulation studies in order to optimize the design. The following data are usually required to design ankle-foot orthoses or prostheses: the joint range of motion (angular position); the mean and maximum values of absolute angular velocity, acceleration, torque, and rotatum; and the frequency response and torque-velocity characteristics of the ankle-foot complex. However, there is no single research work that has assessed all of these parameters.

The effect of muscle weakness on the capability gap during gross motor function is presented in [4]. The paper used maker data and ground reaction forces (GRFs) from several tasks (gait, sit-to-stand, stair ascent, stand-to-sit, and stair descent) to calculate joint kinematics (using inverse kinematics) and estimate joint torques (using inverse dynamics) with OpenSim, where muscle weakness was simulated as reduction in maximal isometric force generation capability of muscles. The exoskeleton was required to provide assist-as-needed by filling the gap between normal and weak muscle conditions. However, once joint torques were estimated for hip, knee, and ankle, the exoskeleton requirements were defined only in terms of *maximum* torques.

The characterization of the ankle joint in the sagittal plane for a range of walking speeds is presented in [5]. The measurements were taken from 10 healthy subjects using speed cameras and a force plate. The ankle parameters were measured for slow, normal and fast gait speeds at three different instances of the gait cycle: controlled plantarflexion, controlled dorsiflexion, and powered plantarflexion. Each subject performed 3 to 9 trials. The final results are not presented in a form that can be readily used for this study but there are data tables for the maximum ankle torque that were quite useful. Another study evaluated the effect of running speed on the lower limb joint kinetics [6]. The data from high speed cameras and a force plate (ground reaction force) were recorded during trials with 8 subjects running at 4 discrete speeds. It was reported that the ankle torque during the stance phase increased from 2.94 Nm/kg to 4 Nm/kg when running speed changed from 3.50 to 8.95 m/s, respectively. Another study related to running along a curve is presented in [7] where 13 human subjects sprinted at maximum effort. The kinematics were recorded using high speed cameras and markers attached to the subjects. Torques of specific joints were estimated by conventional inverse dynamics taking into account ground reaction forces measured by a force plate. The study also included non-sagittal forces, which is useful for designing orthoses and prostheses with more than 1 DoF. Many other studies can

This publication was made possible by NPRP grant No. 6-463-2-189 from the Qatar National Research Fund (a member of The Qatar Foundation). The statements made herein are solely the responsibility of the authors.

A. Gmerek and N. Meskin are with the Department of Electrical Engineering Qatar University, Doha, Qatar, e-mails: {*artur.gmerek*, *nader.meskin*}*@qu.edu.qa*

E. Sobhani Tehrani and R. Kearney are with the Department of Biomedical Engineering, McGill University, Montreal, QC H3A 2B4, Canada, e-mails: *ehsan.sobhani@mail.mcgill.ca*, *robert.kearney@mcgill.ca*

be found especially in the biomechanics literature. However, either they presented only some of the ankle kinematic and dynamic parameters or the results are in a form that cannot be easily used for the design objectives of this paper.

Our motivation for this paper is that a clear and comprehensive quantitative assessment of the ankle-foot kinematics and dynamics required for the design of orthoses is not available in the literature. In general, an artificial ankle joint can be designed to at least partially replicate human ankle kinematics and kinetics during normal walking. Similarly, an active orthosis can be designed such that the mechanical properties of the orthosis combined with those of the patient's ankle mimics the kinematics and kinetics of normal human ankle during upright stance and gait. In addition, both artificial ankle and orthosis shall respond to gait perturbations in a similar way that a normal ankle does, since perturbed gait may occur during daily living due to many factors such as slip, ground irregularities, external forces, etc. This paper provides quantitative assessments of the ankle joint data and dynamics required to establish design requirements for prostheses, orthoses or exoskeletons to achieve the above goals. The main contributions of this paper are:

- Analysis of the frequency domain characteristics of the joint kinematics and kinetics, torque-velocity curve, and torque probability density function.
- Dynamic analysis of the ankle joint compliance, which is the system that an orthosis has to control and a prosthesis to emulate.

This work is focused on the dorsiflexion-plantarflexion degree-of-freedom of the ankle joint, which contributes to movement significantly during walking [8].

This paper is organized as follows. In Section II, the nature of the ankle joint and gait nomenclature are explained. Our methodology is presented in Section III. The assessment of relevant gait studies in the literature is presented in Section IV, which determines the requirements necessary to replicate ankle kinematics and kinetics during walking. Section V provides the assessment of the ankle joint dynamic stiffness model, which determines mostly the requirements to withstand gait perturbations. The results are discussed in Section VI and conclusions are stated in Section VII.

II. The characteristics of the ankle joint and gait

In simple terms, the ankle joint is a hinge between the shank and the foot. In the medical literature, it is known as the talocrural region that includes three joints: talocrural, subtalar, and inferior tibiofibular [9]. The main bones of the ankle joint are tibia and fibula (in the shank) and talus (in the foot), which are connected by ligaments and articulated by muscles. Almost all leg muscles below the knee contribute to the ankle movement but their functional roles differ depending on cadence, direction of motion, and individual features of a subject [10]. The PF movement is mostly controlled by the gastrocnemius, soleus, and peroneus longus muscles. The DF movement is controlled by tibialis anterior, extensor digitorium longus, and extensor hallucis longus muscles. The gastrocnemius and soleus muscles are connected to the bone via the Achilles tendon.

The ankle joint produces movement mainly in the dorsiflexion-plantarflexion (DF/PF) direction. Also, the subtalar joint of the ankle allows inversion-eversion of the foot during movement [11]. Each gait cycle consists of two phases: stance phase where the foot maintains contact with the ground, and swing phase corresponding to the time when the foot is in the air. The stance phase can be further divided into five sub-phases: initial contact, loading response, mid-stance, terminal stance, and pre-swing; the swing phase can be divided into initial swing, mid-swing, and terminal swing [12].

Sensors such as potentiometers, encoders, IMU sensors, and goniometers can be used to record ankle angular position. The ankle position can also be estimated using scanners or by recording the position of the foot with cameras. In the latter case, markers are placed on the foot and shank to facilitate the image processing algorithms. Measuring ankle torque during walking is complicated due to redundancy in human motor control system. Also, it is very difficult to measure the forces produced by the muscles articulating the ankle joint since sensors shall be placed inside the human organism. Therefore, currently the most common approach to estimate joint torques is to record the GRFs and then apply the inverse dynamics procedure using a model of the multi-joint body segments. This method was shown to provide good accuracy [13].

III. Methodology

The results presented in this study are obtained using (a) *OpenSim* application [14] and (b) MATLAB for processing experimental data collected from the peer-reviewed articles. Using *OpenSim* we were able to combine data from different sources, process the data, and apply the inverse kinematics and dynamics procedures. Thus, in one case study, we used the time history of the ankle joint from [15] using the *OpenSim* simulation files and associated datasets that the authors provided. However, we could not find sufficiently comprehensive databases that covered the full spectrum of walking experiments and requirements. Therefore, we considered several studies summarized in Tables I and II to obtain more data. These tables show data sources and studies that were maintained after removing the sources with outlier observations. It should be noted that these data sources contained only ankle position and torque. Thus, we used numerical differentiation to calculate rotatum and angular velocity and acceleration, where the derivatives were approximated by the conventional Taylor series expansion with central difference where only the 1^{st} term was included. Finally, we obtained the absolute values of the numerically calculated ankle angular velocity, acceleration and rotatum.

The second part of our quantitative assessment was based on the dynamic stiffness model of the ankle joint developed in REKLAB, which defines the dynamic relationship between ankle angular position and the torque acting about it. The stiffness model consists of two components: *intrinsic* and *reflex*. The intrinsic stiffness arises from the mechanical properties of the joint, passive tissue, and active

TABLE I. THE SOURCES USED FOR EXTRACTING KINEMATICS DATA (THE GAIT CYCLE WAS 1.2 SECONDS)

source	information
[16]	The time history of the ankle joint angle from a stimulation study. Authors studied the effect of cadence regulation on muscle activation. The data are taken from the plot of a gait cycle versus angle.
[17]	Authors presented the average ankle angle plots of 16 subjects, which was extracted for our study.
[18]	This was a paper on the control of a powered ankle-foot prosthesis. The plot of the prosthesis angle tracking over one gait cycle was provided. The data were measured by prosthesis sensors.
[15]	This was a study on the stabilization of walking by intrinsic muscle properties. The data were extracted from the plot of ankle angle for one subject.
[19]	The authors presented a plot of the ankle angle for 1 healthy subject, which is used in our study.

TABLE II. THE SOURCES USED FOR EXTRACTING ANKLE TORQUE DATA

source	information	subject's mass [kg]
[16]	The data are extracted from the time history of ankle torque (Nm/kg) for one subject. Authors studied the effect of cadence regulation on muscle activation.	-
[17]	The authors presented a plot of the average ankle torques in 16 subjects as a function of gait cycle. Torque is given in units of (Nm/kg).	-
[18]	The data are extracted from the plot of prosthesis torque tracking over one gait cycle. The torque is estimated from a series elastic actuation system.	75
[15]	The study of stabilizing walking with intrinsic muscle properties. The plot of the torque from one subject was used (*OpenSim* simulation data).	72.6
[20]	The plot of ankle torque for a healthy subject walking at maximum velocity. The paper presented a mechanical model to study the relationship between gait velocity and muscular strength. The torque calculated based on the inverse dynamics model. No information about exact weight of the subject was given (numbers varied between 48kg to 72.6kg; thus we used the mean value of 61.1kg).	61.1

muscle fibers. The reflex stiffness component arises from the changes in muscle activation due to the afferent response to the stretch of muscles [21]. The experimental procedure to identify the stiffness model was to apply pseudo-random perturbations to the ankle, while the foot was placed in the custom-fitted boot attached to an electro-hydraulic actuator [22], and ankle position, torque and EMG signals were recorded. A nonlinear, parallel-cascade system identification method was used to identify both intrinsic and reflex ankle stiffness from recorded data [23].

The stiffness model was used to analyze the dynamics of the ankle-foot complex and to derive its torque-velocity curve. The parallel-cascade structure of the intrinsic and reflex stiffness is shown in Fig. 1. The intrinsic stiffness is represented by a second-order inertia, damping, and elasticity model with parameters I, B, and K. The reflex stiffness was modeled by a velocity sensitive Hammerstein system consisting of a nonlinear half-wave rectifier followed by a second order linear dynamics with parameters G, ζ and ω that represent reflex gain, damping and natural frequency, respectively. The reflex response has a delay of 40ms due to the stretch reflex arc.

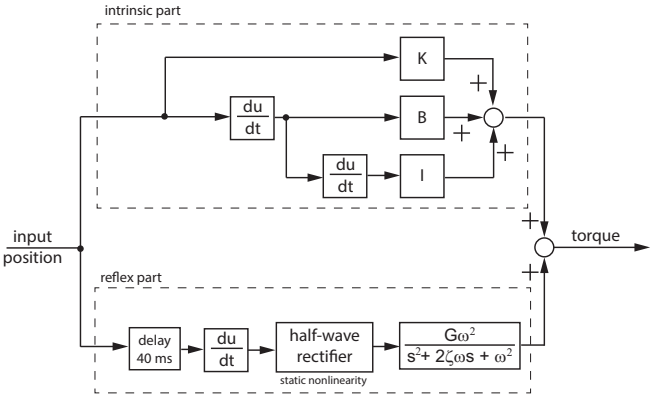

Fig. 1. The block diagram of the parallel-cascade model of the ankle joint dynamic stiffness including intrinsic and reflex components.

IV. ASSESSMENT OF THE RESULTS OF THE GAIT STUDIES

The parameters calculated from the data sources (or gait studies) in Tables I and II are summarized in Tables III and IV. The references [15] - [18] provide both ankle position and torque signals, which were used to obtain the amplitude spectrum and the torque-velocity curve during gait. First, the data were preprocessed to align the gait cycles to start from approximately the same position (Figure 2). Then, the frequency analysis was performed on the aligned data. As can be observed from Figure 3, the major frequency components are below 5Hz (i.e., low frequency). A small fraction appears in the higher frequency range, which is most likely related to the heel strike phase of walking.

Figure 4 shows the torque-velocity scatter plot during walking with the dashed lines (in purple) representing the encompassing curve. Figure 5 shows probability density function (PDF) of the mean torque from sources presented in Table IV. By integrating the area underneath the PDF curve ($P = \int_{\tau_1}^{\tau_2} p(\tau)d\tau$) it is possible to approximate the probability of torque occurring within some specific range, and based on this information optimize the selection of an actuator. For example, during normal walking with a gait cycle of 1.2s, the required torque is less than 0.2 Nm/kg for about 0.6s (half of the cycle). The large torques (i.e. larger than 1.1 Nm/kg) are required for only 0.12s, which is only 10% of the gait cycle. This information is important when using an electric actuator to drive an artificial ankle joint or an orthosis since most electric motors can supply large torques for only a limited period of time.

TABLE III. THE RESULTS OF THE KINEMATIC DATA PROCESSING: MINIMUM POSITION, MAXIMUM POSITION, RANGE OF MOTION, MEAN ABSOLUTE VELOCITY, MAXIMUM ABSOLUTE VELOCITY, MEAN ACCELERATION, MEAN ABSOLUTE ACCELERATION, AND MAXIMUM ABSOLUTE ACCELERATION.

source	$\alpha_{\min}$ [deg]	$\alpha_{\max}$ [deg]	ROM [deg]	$v_{\text{mean abs}}$ [deg/s]	$v_{\max \text{ abs}}$ [deg/s]	a_{mean} [deg/s^2]	$a_{\text{mean abs}}$ [deg/s^2]	$a_{\max \text{ abs}}$ [deg/s^2]
[16]	-17.9	8.9	26.8	52.4	206.1	34.4	967	4322
[17]	-17.1	10.8	28.0	54.6	177.4	37.4	810	4074
[18]	-19.3	11.8	31.1	61.3	265.5	68.2	963	5043
[15]	-8.6	14.2	22.8	46.3	249.6	26.6	883	5874
[19]	-16.5	4.3	20.8	42.0	211.4	45.4	733	4261
mean	-15.88	11.16	27	52.74	222	42.4	871.2	4714.8

TABLE IV. THE RESULTS OF PROCESSING TORQUE DATA: MAXIMUM TORQUE, MEAN TORQUE, MEAN ROTATUM, AND MAXIMUM ROTATUM. DATA WERE WEIGHTED ACCORDING TO THE NUMBER OF SUBJECTS IN EACH STUDY.

source	$\tau_{\max}$ [Nm/kg]	$\tau_{\text{mean abs}}$ [Nm/kg]	$P_{\text{mean abs}}$ [Nm^2/(kg.s)]	$P_{\max \text{ abs}}$ [Nm^2/(kg.s)]
[16]	1.7	0.5	3.0	22.9
[17]	1.5	0.5	3.0	12.0
[18]	1.6	0.5	3.6	21.5
[15]	1.8	0.5	3.3	16.2
[20]	2.0	0.6	3.3	18.9
mean (weighted)	1.84	0.55	3.26	18.56

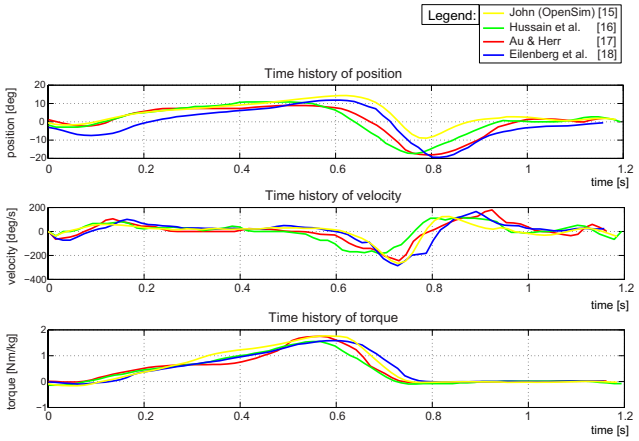

Fig. 2. The time history of ankle angular position, velocity and torque during walking.

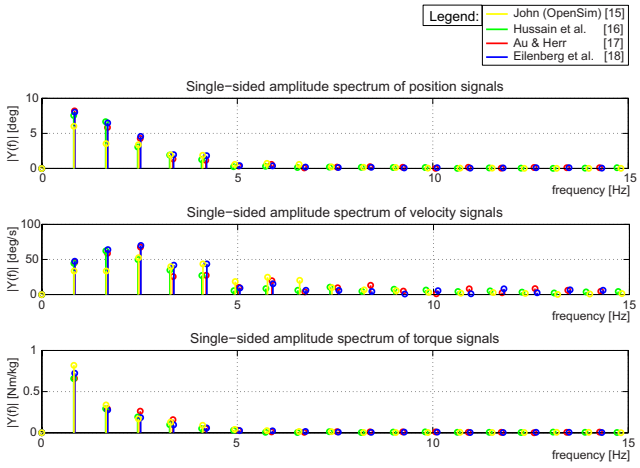

Fig. 3. The single-sided *amplitude* spectrum of ankle angular position, velocity and torque during walking (Note that the mean of the signals were removed before FFT calculations of the amplitude spectrum).

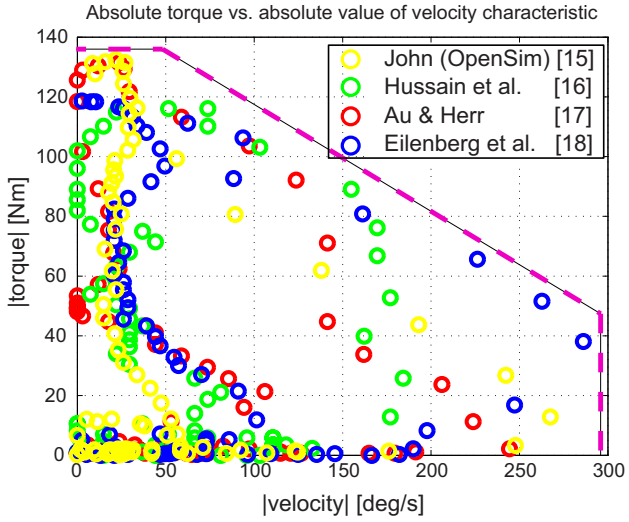

Fig. 4. The torque-velocity characteristic during walking for a 75 kg subject. To emulate normal human ankle joint, the torque-velocity characteristic of an actuator must be above the purple dashed line.

V. THE ANALYSIS OF THE ANKLE STIFFNESS MODEL

In the previous section, the assessment of the ankle joint kinematic and kinetic data from several gait studies was presented. In this section, the ankle joint dynamic stiffness model is analyzed to derive design requirements for an orthotic device intended to assist patients during walking, who have altered intrinsic and/or reflex stiffness properties at the ankle due to a neuromuscular disease. The input to the stiffness model (i.e. the ankle position) should be a signal that evokes proprioceptive reflexes in a wide frequency range. The maximum ankle angular velocity was chosen as 246 deg/s, which corresponds to the velocity of an average magnitude slip [24] (see also [25]). Other parameters of the stiffness model are given in Table V. The ankle intrinsic and reflex stiffness parameters change as a

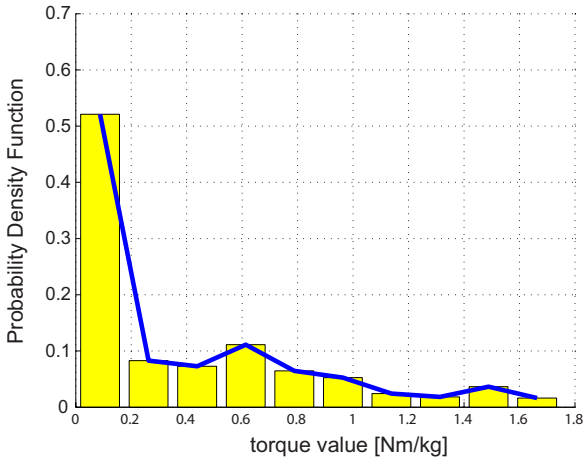

Fig. 5. The probability density function of ankle torque during walking with 1.2s gait cycle, obtained from sources in Table IV.

TABLE V. THE PARAMETERS OF THE STIFFNESS MODEL BASED ON WHICH THE TORQUE-VELOCITY CURVE AND THE FREQUENCY RESPONSE OF THE ANKLE WERE OBTAINED.

parameter	value
I	0.0131 $\frac{\text{Nm.s}^2}{\text{rad}}$
K	500 $\frac{\text{Nm}}{\text{rad}}$
B	2 $\frac{\text{Nm.s}}{\text{rad}}$
G	100 $\frac{\text{Nm.s}}{\text{rad}}$
ω	8.285 $\frac{\text{rad}}{s}$
ζ	0.412

function of ankle angle and muscle activation. The parameter values in Table V correspond to the largest feasible intrinsic stiffness (K) and reflex gain (G) in majority of normal [21] (and even pathological [26]) subjects. Typically, the largest intrinsic gain (K) occurs at dorsiflexed ankle position and when muscle activations are large. The largest reflex gain (G) occurs at dorsiflexed position with small (but non-zero) muscle activations. torques at the ankle. The time history of the input position perturbation, the corresponding perturbation velocity, and the output torque of the stiffness model is shown in Figure 6. Moreover, Figure 7 shows the corresponding torque-velocity characteristic. Note that the inertial torque of the foot were not taken into account for characterizing the torque-velocity curve. An orthosis can be designed to counteract the mass (or inertia) related effects of gravity in patient with foot drop by providing a static force support. However, our orthosis design concept does not require *actively* changing the inertia of the ankle-foot complex. Rather, we intend to use the orthosis to actively change the elasticity, damping and reflex gain of the wearer's ankle. Thus, we excluded inertial torques from torque-velocity characterization.

Figure 7 shows the torque-velocity scatter plot obtained from the parallel-cascade stiffness model simulation. The torque-velocity curve of an orthosis (or prosthesis) actuator must be above (a) the red dashed line in Figure 7 to emulate

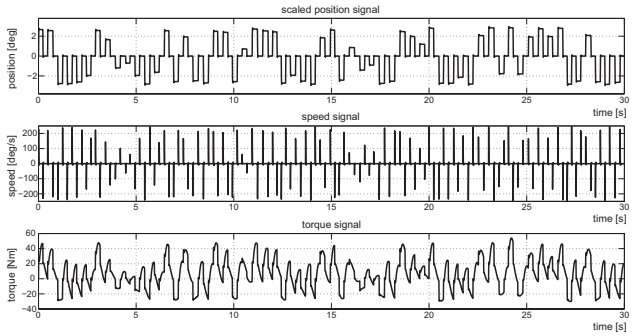

Fig. 6. The input position perturbation, the corresponding perturbation velocity, and the output torque response of the parallel-cascade ankle joint stiffness model.

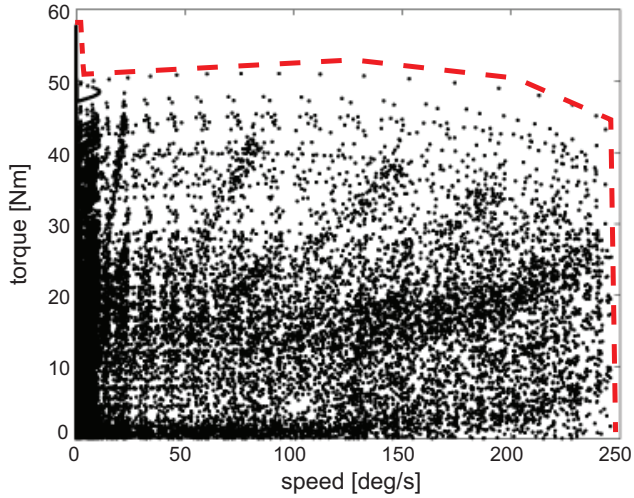

Fig. 7. The torque-velocity scatter plot obtained from the parallel-cascade stiffness model simulation. To emulate the ankle joint, the torque-velocity curve of an orthosis actuator must be above the red dashed line.

human ankle dynamics and (b) the purple dashed line in Figure 4 to emulate ankle kinematics and kinetics during gait. This requirement is most likely feasible for hydraulic or pneumatic actuators but it is more difficult to fulfill using electric actuators due to their generally lower torque to mass ratios.

The ankle compliance, which is the inverse of stiffness, is the system that the orthosis has to assist and control (cooperatively with the central nervous system) since orthosis torque is applied to the ankle as input and the resulting ankle position is the output. Therefore, the ankle compliance model shown in Figure 8 was used to calculate the bandwidth of the ankle joint. It was assumed that the ankle compliance model has the same parameter values as those presented for stiffness in Table V. As mentioned previously, the values of these parameters depend on the ankle position and voluntary muscle contraction. However, we did not consider these dependencies in this study and used a worst-case analysis approach. The presence of the half-wave rectifier nonlinearity in the reflex pathway does not allow using conventional methods of frequency response calculation [27], [28]. Thus, to estimate the ankle bandwidth,

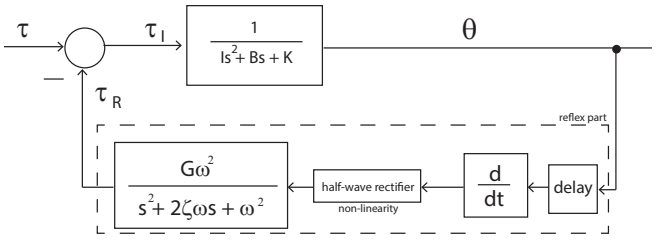

Fig. 8. The ankle compliance model, the inverse of stiffness, that was used to calculate the ankle bandwidth.

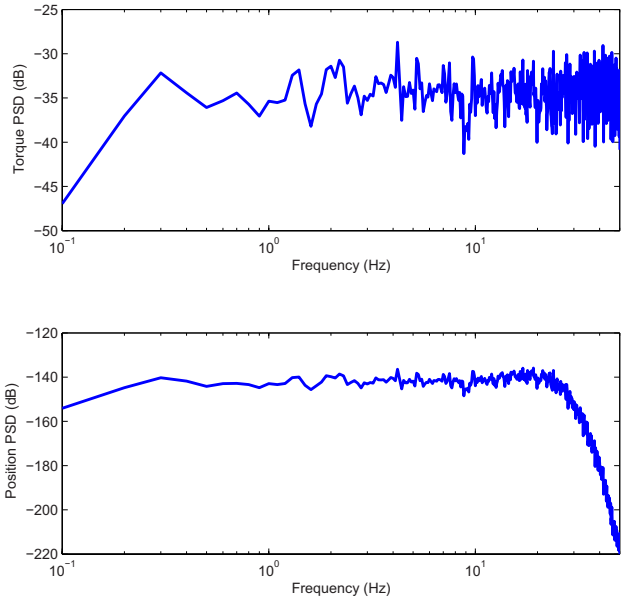

Fig. 9. The PSD estimate of the input torque (top) and output position (bottom) of the ankle compliance model in response to a white input torque.

the ankle compliance model was driven by a pseudo-random white input torque and the power spectral density (PSD) of the output position was calculated. The estimated PSD of the input and output is shown in Figure 9. The figure indicates that the ankle compliance dynamics will respond to torque perturbations (or external inputs) up to 25Hz and any torque perturbations above 25Hz will be significantly attenuated. Consequently, the ankle compliance bandwidth is about 25Hz. A robot required to fully emulate the dynamic properties of the ankle joint compliance must have similar bandwidth. However, a 5Hz bandwidth is sufficient for most *unperturbed* activities of daily living such as normal walking.

VI. Discussion

In the first part of this paper, we presented the results of processing gait data from several peer-reviewed articles. In this section, we further discuss the meaning and significance of some of the results. For example, using the amplitude spectrum of position and torque from a gait cycle (Figure 3), we determined that the *functional* bandwidth of the ankle joint during normal gait is almost 5Hz. This finding is somewhat consistent with the work presented in [17], where

TABLE VI. The summary of the study

parameter	meaning	mean value [unit]
$\alpha_{\min}$	max. platarflexion position	-15.88 [deg]
$\alpha_{\max}$	max. dorsiflexion position	11.16 [deg]
ROM	range of motion	27 [deg]
$v_{\text{mean abs}}$	mean absolute speed	52.74 [deg/s]
$v_{\max\text{ abs}}$	max. absolute speed	222 [deg/s]
$a_{\text{mean abs}}$	mean absolute acceleration	871.2 [deg/s^2]
$a_{\max\text{ abs}}$	max. absolute acceleration	4714.8 [deg/s^2]
$\tau_{\text{mean abs}}$	mean absolute torque	0.55 [Nm/kg]
$\tau_{\max}$	max. absolute torque	1.84 [Nm/kg]
$P_{\text{mean abs}}$	mean absolute rotatum	3.26 [Nm^2/kg.s]
$P_{\max\text{ abs}}$	max. absolute rotatum	18.56 [Nm^2/kg.s]
frequency bandwidth	5 [Hz] (based on the gait data) up to 25 [Hz] (based on the stiffness model)	

the bandwidth estimated from the power spectrum of the ankle torque during the stance phase of walking was 3.5Hz.

The second part of the paper is the main novelty of this work, where we simulated and analyzed the parallel-cascade model of ankle joint stiffness to determine the *dynamic* bandwidth of the ankle in response to external inputs and perturbations. We found this bandwidth to be almost 25Hz. This is a very demanding requirement for orthoses and prostheses actuators where stringent constraints exist for the mass of the device. Therefore, most of these devices do not meet this criteria.

The torque-velocity requirements were derived based on (a) data from gait studies (Figure 4) and (b) simulated data from the parallel-cascade joint stiffness model (Figure 7). The gait torque-velocity requirement was derived from the scatter plot of ankle torque and velocity at an average gait speed. The torque-velocity requirement obtained from the stiffness model simulation corresponded to a maximum perturbation speed of 246 deg/s to prevent an average magnitude slip during gait. Also, the torque-velocity characteristics revealed the natural tendency of the muscles to generate greater torques with lower ankle angular velocities. Similar results are also presented in an experimental study of the ankle joint [29].

VII. Conclusions

The paper presented the kinematics, kinetics and dynamic system properties of the ankle joint in the sagittal plane (DF/PF) based on the analysis of experimental data from several gait studies and simulated data of the parallel-cascade model of ankle intrinsic and reflex stiffness. The main outcomes of our quantitative assessments are presented in Tables III and IV and are summarized in Table VI. Additional requirements for the ankle frequency response (or bandwidth) during gait is given in Figure 3, the torque-velocity curves in Figures 4 and 7, and the PDF of torque during gait in Figure 5. The presented data is very useful for designing artificial ankle joints, prostheses, and rehabilitation and assistive robots (or orthoses). In fact, we have used this data to develop an ankle-foot orthosis (AFO) that is intended to assists patients with neuromuscular disorder by modulating the intrinsic and/or reflex stiffness of the ankle.

REFERENCES

[1] R. L. Martin, T. E. Davenport, S. Paulseth, D. K. Wukich, J. J. Godges, R. D. Altman, A. Delitto, J. DeWitt, A. Ferland, H. Fearon *et al.*, "Ankle stability and movement coordination impairments: ankle ligament sprains: clinical practice guidelines linked to the international classification of functioning, disability and health from the orthopaedic section of the american physical therapy association," *Journal of Orthopaedic & Sports Physical Therapy*, vol. 43, no. 9, pp. A1–A40, 2013.

[2] Annual statistical report 2014. National Spinal Cord Injury Statistical Center. [Online]. Available: www.nscisc.uab.edu

[3] The amputee coalition of america. [Online]. Available: www.amputee-coalition.org

[4] M. Afschrift, F. De Groote, J. De Schutter, and I. Jonkers, "The effect of muscle weakness on the capability gap during gross motor function: a simulation study supporting design criteria for exoskeletons of the lower limb," *Biomedical engineering online*, vol. 13, no. 1, p. 111, 2014.

[5] M. L. Palmer, "Sagittal plane characterization of normal human ankle function across a range of walking gait speeds," Ph.D. dissertation, Citeseer, 2002.

[6] A. G. Schache, P. D. Blanch, T. W. Dorn, N. Brown, D. Rosemond, and M. G. Pandy, "Effect of running speed on lower limb joint kinetics," *Med Sci Sports Exerc*, vol. 43, no. 7, pp. 1260–1271, 2011.

[7] G. Luo and D. Stefanyshyn, "Limb force and non-sagittal plane joint moments during maximum-effort curve sprint running in humans," *The Journal of experimental biology*, vol. 215, no. 24, pp. 4314–4321, 2012.

[8] K. E. Zelik, K. Z. Takahashi, and G. S. Sawicki, "Six degree-of-freedom analysis of hip, knee, ankle and foot provides updated understanding of biomechanical work during human walking," *The Journal of experimental biology*, vol. 218, no. 6, pp. 876–886, 2015.

[9] K. L. Moore, A. F. Dalley, and A. M. Agur, *Clinically oriented anatomy*. Lippincott Williams & Wilkins, 2013.

[10] N. J. Cronin, J. Avela, T. Finni, and J. Peltonen, "Differences in contractile behaviour between the soleus and medial gastrocnemius muscles during human walking," *The Journal of experimental biology*, vol. 216, no. 5, pp. 909–914, 2013.

[11] A. Lundberg, O. Svensson, G. Nemeth, and G. Selvik, "The axis of rotation of the ankle joint," *Journal of Bone & Joint Surgery, British Volume*, vol. 71, no. 1, pp. 94–99, 1989.

[12] J. Perry, J. M. Burnfield, and L. M. Cabico, "Gait analysis: normal and pathological function," 1992.

[13] G. Robertson, G. Caldwell, J. Hamill, G. Kamen, and S. Whittlesey, *Research methods in biomechanics, 2E*. Human Kinetics, 2013.

[14] S. Delp, F. Anderson, A. Arnold, P. Loan, A. Habib, C. John, E. Guendelman, and D. Thelen, "Opensim: Open-source software to create and analyze dynamic simulations of movement," *IEEE Transactions on Biomedical Engineering*, vol. 54, no. 11, pp. 1940–1950, 2007.

[15] C. T. John, F. C. Anderson, J. S. Higginson, and S. L. Delp, "Stabilisation of walking by intrinsic muscle properties revealed in a three-dimensional muscle-driven simulation," *Computer methods in biomechanics and biomedical engineering*, vol. 16, no. 4, pp. 451–462, 2013.

[16] S. Hussain, S. Xie, and P. Jamwal, "Effect of cadence regulation on muscle activation patterns during robot-assisted gait: A dynamic simulation study," *IEEE Journal of Biomedical and Health Informatics*, vol. 17, no. 2, pp. 442–451, 2013.

[17] S. K. Au and H. Herr, "Powered ankle-foot prosthesis," *Robotics & Automation Magazine, IEEE*, vol. 15, no. 3, pp. 52–59, 2008.

[18] M. Eilenberg, H. Geyer, and H. Herr, "Control of a powered ankle–foot prosthesis based on a neuromuscular model," *IEEE Transactions On Neural Systems And Rehabilitation Engineering*, vol. 18, no. 2, pp. 164–173, 2010.

[19] D. Li, A. Becker, K. A. Shorter, T. Bretl, and E. Hsiao-Wecksler, "Estimating system state during human walking with a powered ankle-foot orthosis," *Mechatronics, IEEE/ASME Transactions on*, vol. 16, no. 5, pp. 835–844, 2011.

[20] S. Nadeau, D. Gravel, A. Arsenault, and D. Bourbonnais, "A mechanical model to study the relationship between gait speed and muscular strength," *IEEE Transactions on Rehabilitation Engineering*, vol. 4, no. 4, pp. 386–394, 1996.

[21] M. Mirbagheri, H. Barbeau, and R. Kearney, "Intrinsic and reflex contributions to human ankle stiffness: variation with activation level and position," *Experimental Brain Research*, vol. 135, no. 4, pp. 423–436, 2000.

[22] R. Kearney, R. Stein, and L. Parameswaran, "Identification of intrinsic and reflex contributions to human ankle stiffness dynamics," *IEEE Transactions on Biomedical Engineering*, vol. 44, no. 6, pp. 493–504, 1997.

[23] D. Ludvig, T. Visser, H. Giesbrecht, and R. Kearney, "Identification of time-varying intrinsic and reflex joint stiffness," *IEEE Transactions on Biomedical Engineering*, vol. 58, no. 6, pp. 1715–1723, 2011.

[24] P. F. Tang, M. H. Woollacott, and R. K. Y. Chong, "Control of reactive balance adjustments in perturbed human walking: roles of proximal and distal postural muscle activity," *Exp Brain Res*, no. 119, pp. 141–152, 1998.

[25] R. R. Ferber, "Gait perturbation response in anterior cruciate ligament deficiency and surgery," Ph.D. dissertation, Department of Exercise and Movement Science, University of Oregon, 2001.

[26] M. Mirbagheri, H. Barbeau, M. Ladouceur, and R. E. Kearney, "Intrinsic and reflex stiffness in normal and spastic, spinal cord injured subjects," *Exp Brain Res*, vol. 141, no. 4, pp. 446–459, 2001.

[27] A. Pavlov, N. van de Wouw, and H. Nijmeijer, "Frequency response functions and bode plots for nonlinear convergent systems," in *Decision and Control, 2006 45th IEEE Conference on*. IEEE, 2006, pp. 3765–3770.

[28] J. Lataire, R. Pintelon, and E. Louarroudi, "Non-parametric estimate of the system function of a time-varying system," *Automatica*, vol. 48, no. 4, pp. 666–672, 2012.

[29] D. G. Thelen, "Adjustment of muscle mechanics model parameters to simulate dynamic contractions in older adults," *Journal of biomechanical engineering*, vol. 125, no. 1, pp. 70–77, 2003.